

BAND CONTOUR CALCULATIONS AND *l*-DOUBLING EFFECTS IN SYMMETRIC TOP VIBRATION-ROTATION SPECTRA

IAN M. MILLS

Department of Chemistry, University of Reading, Reading, U.K.

In this lecture I plan to discuss three aspects of our recent work on the analysis of high resolution rotation-vibration spectra. The first concerns the value of using computer-calculated band contours (or computer-simulated spectra) for the analysis of rotation-vibration structure in the band spectra of heavy molecules, in situations where the structure is only partially resolved. The second concerns the origin and importance of *l*-doubling interactions (and *xy* axis Coriolis interactions) in the observed rotational structure of symmetric top molecules. I shall demonstrate that, at least in certain cases, *l*-doubling effects produce considerable modifications to the observed band contours of symmetric top molecules. The third subject which I wish to discuss briefly concerns the theoretical treatment of the complete rovibrational Hamiltonian by means of a Van Vleck or contact transformation. This provides the best method of understanding *l*-doubling interactions. I shall also present new results, mainly for infrared spectra of cyclopropane, illustrating this work.

I should like to start by recalling the spectrum of the CH₃F molecule in the 1460 cm⁻¹ region, which is illustrated in the lower half of *Figure 1*. This spectrum was analysed recently by Dr. di Lauro, working in my laboratory¹; he demonstrated that the curious appearance of this spectrum is due to the fact that there are two accidentally coincident fundamentals of the molecule within 10 cm⁻¹ of each other, which are interacting through an *xy* axis type of Coriolis perturbation. The fundamentals are an *A*₁ species parallel band, ν_2 at 1460.0 cm⁻¹, and an *E* species perpendicular band, ν_5 at 1468.0 cm⁻¹. The strong Coriolis interaction between these bands, due to the $\zeta_{2,5}^{(x,y)}$ Coriolis constant, produces perturbations of the true energy levels and wavefunctions which result in the *J* structure of the *Q* branches of the perpendicular band apparently degrading in opposite directions in the high frequency and low frequency wings of the band, and which also result in the very curious appearance of the *Q* branch of the parallel band close to 1460 cm⁻¹. The upper half of *Figure 1* shows computer-calculated band contours for this pair of bands, based on a model in which the interaction has been correctly allowed for in its effect on the positions and intensities of all lines in the spectrum.

The advantage of this technique is that the computer can be programmed to set up and diagonalize a Hamiltonian matrix numerically, without approximation, despite the fact that it is not possible to obtain analytical expressions for the line positions and intensities. Moreover, the computed

band contour (obtained directly from a graph plotter linked on-line to the computer) can be directly compared to the observed spectrum despite the fact that the resolution is insufficient to allow a complete assignment and analysis of the rotational structure. The difference between the computed spectra (a) and (b) shows the advantage of accurate intensity calculations:

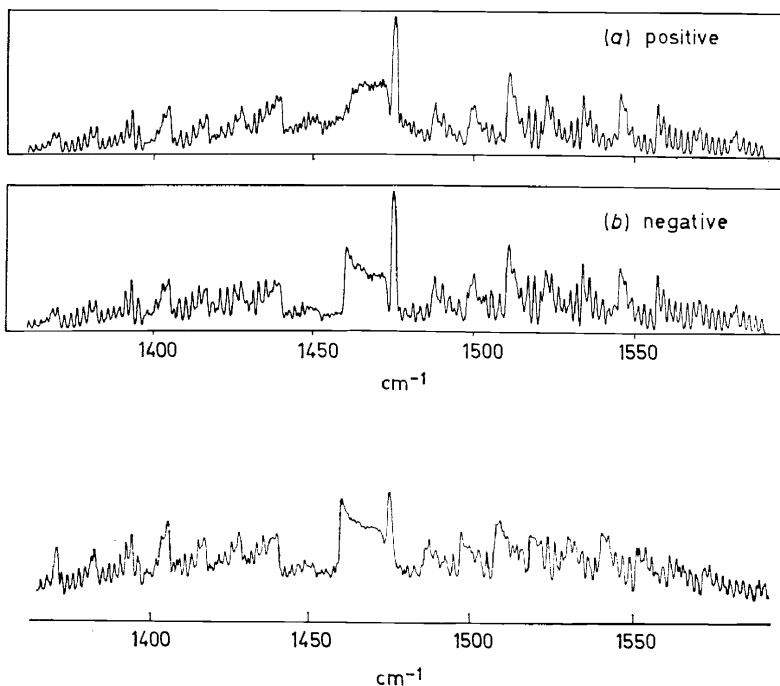


Figure 1. Observed and computed spectra for CH_3F near 1460 cm^{-1}

the two spectra differ in the relative sense assumed for the dipole moment derivatives ($\partial\mu^z/\partial Q_2$) and ($\partial\mu^{x,y}/\partial Q_{5a,b}$), and it is possible to see at once that the computed spectrum (b) represents the true state of affairs in the molecule rather than the spectrum (a). This leads to the experimental determination of the sign relation between the dipole moment derivatives which is illustrated in Figure 2 (see also reference 1).

Figure 3 shows an interaction diagram for the energy levels, illustrating the origin of this perturbation. The diagram shows rotational energy levels of different K but the same value of J (' K -Stacks') for each of three different vibrational levels: the ground vibrational state, species A_1 ; the excited parallel vibrational state, species A_1 ; and the excited perpendicular vibrational state, species E . Typical xy axis Coriolis interactions are indicated by the broken lines connecting levels satisfying the selection rules $\Delta k = \Delta l = \pm 1$, between the two excited vibrational states[†]. Solid lines indicate typical

[†] I use k and l as signed quantum numbers for the component of total angular momentum and vibrational angular momentum in the top axis respectively, and I use $K = |k|$ (see Herzberg², p. 24).

BAND CONTOUR AND *l*-DOUBLING EFFECTS

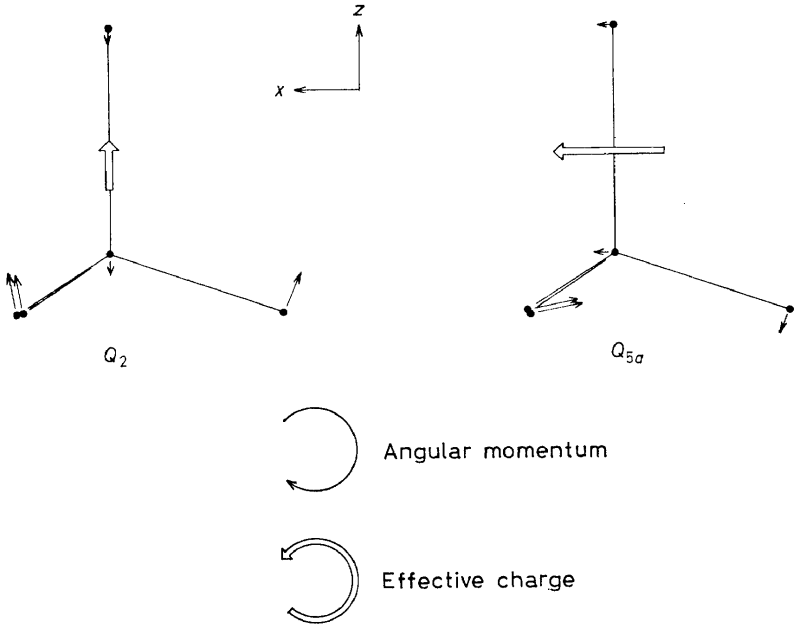


Figure 2. Sign relationship between dipole moment derivatives in CH_3F

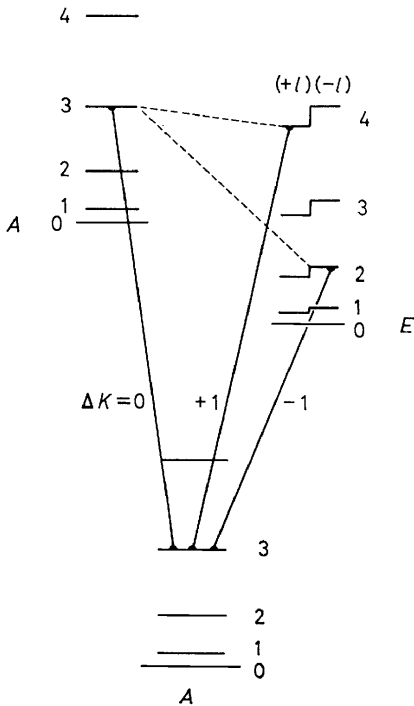


Figure 3. Energy level interaction diagram for an *A* and *E* species vibrational level interacting through an *xy* axis Coriolis term

allowed transitions in the two bands. It will be seen that the perturbation mixes together three upper state wavefunctions to which transitions are allowed from the same ground state wavefunction; hence the positions and intensities of all three lines become mutually perturbed. The Hamiltonian matrix for this interaction factorizes into (3×3) blocks, corresponding to three levels connected by the interaction as indicated in *Figure 3*.

A typical (3×3) block of the Hamiltonian matrix is shown diagrammatically in the upper half of *Figure 4*. The diagonal elements in this matrix represent the usual symmetric top rotation-vibration energy levels of the unperturbed Hamiltonian, in which v_s and v_t denote A_1 and E species vibrations respectively,

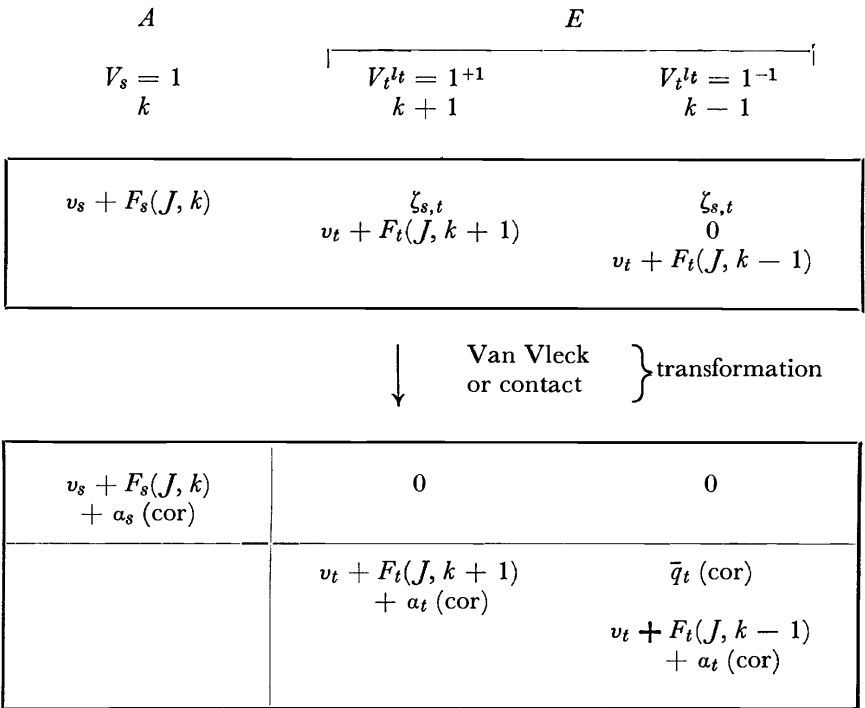


Figure 4. Diagrammatic representation of the effect of a Van Vleck transformation to remove cross terms between different vibrational levels

$$F_s(J, k) = B_s J(J + 1) + (A_s - B_s)k^2$$

and

$$F_t(J, k) = B_t J(J + 1) + (A_t - B_t)k^2 \mp 2A_t \zeta_{ta, tb}^{(2)} k$$

The interaction terms are only indicated diagrammatically; they depend on the xy axis zeta constant connecting the two vibrations, and are given by the expression

$$(2)^{\frac{1}{2}} B_t \zeta_{s, ta}^{(y)} [J(J + 1) - k(k \pm 1)]^{\frac{1}{2}}$$

Consider now the more general situation that the vibrational energies ν_s and ν_t are very different, so that there is no longer a near accidental degeneracy between parallel and perpendicular bands. We now have the situation that two nearly degenerate energy levels in the E vibrational state, characterized by

$$|l_t = +1, k + 1\rangle \text{ and } |l_t = -1, k - 1\rangle$$

are indirectly connected through the remote energy level characterized by

$$|l_t = 0, k\rangle$$

in the A_1 vibrational state. We can allow for the effect of such cross-terms by a development of second-order perturbation theory, known as a Van Vleck (or contact) transformation³, according to which we transform the Hamiltonian matrix into a new representation in which there are no cross-terms between the different vibrational states ν_s and ν_t , but instead there are correction terms to the diagonal elements of the matrix, and also a cross-term between the two nearly degenerate levels of the type:

$$H_{23} = H_{21} H_{13}/\Delta$$

where $\Delta = (\nu_s - \nu_t)$. The effect of the transformation in this case is shown diagrammatically in the lower half of *Figure 4*, where it can be seen that the interaction term between the nearly degenerate levels in the perpendicular band has been labelled \bar{q}_t (cor): it is this term which represents the l -type doubling interaction in the rotational levels of the degenerate vibrational state. Again *Figure 4* is diagrammatic. The exact expressions for the terms in the transformed Hamiltonian are given below.

The Van Vleck transformation to remove cross terms between different vibrational levels leaves us with a separate effective Hamiltonian matrix for each vibrational level. The transformation may be thought of as a separation of vibration from rotation, equivalent to the familiar Born–Oppenheimer separation of electronic from vibrational degrees of freedom to give an effective Hamiltonian for the nuclear motion in each electronic state.

The constant \bar{q} is known as the l -doubling interaction constant[†], and is characteristic of the particular degenerate vibrational state. *Figure 5* shows a K -stack of rotational energy levels (all characterized by the same value of J) in the degenerate vibrational state. The l -doubling interactions are shown as dotted lines between appropriate pairs of energy levels. It will be seen that the l -doubling interactions satisfy the selection rule

$$\Delta k = \Delta l_t = \pm 2$$

In general these cross terms connect levels of a different rotational energy, and since typical values of the constant \bar{q} are of the order of the rotational constant α , representing the vibrational dependence of B , the effect of the cross terms may often be neglected. However, for the $k = l = \pm 1$ pair of levels, the cross term produces an interaction between two states which would otherwise be degenerate, and in consequence mixes the wavefunctions 50/50

[†] The symbol \bar{q} is used for the l -doubling constant; the significance of the bar is merely to distinguish it from the symbol for a dimensionless normal coordinate, since q is already a somewhat overworked symbol.

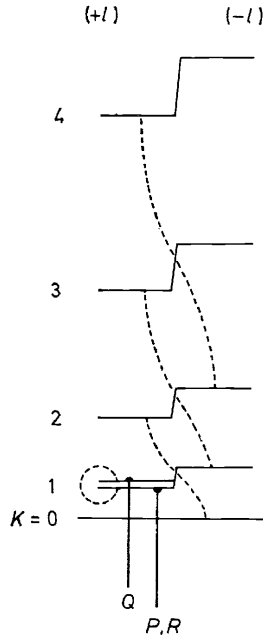


Figure 5. Interaction diagram for l -doubling in an E vibrational level

and splits the energy levels apart by the magnitude of the interaction term. This produces a perturbation of the ${}^R Q_0$ sub-band such that the Q branch transitions go to one of the two energy levels and P and R branch transitions to the other, with the result that the effective B values in the Q branch and the P and R branches of the ${}^R Q_0$ sub-band are different. This effect of the l -doubling interaction is well known.

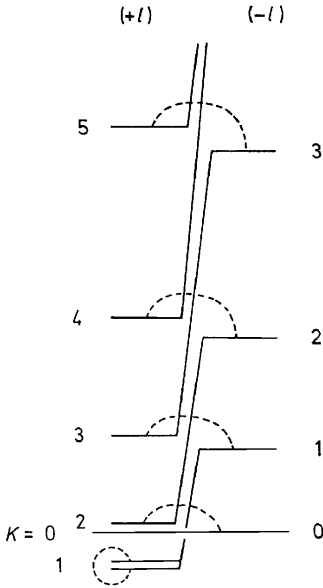
The other cross terms, which are normally neglected, can become important if the diagonal zeta constant $\zeta_{ta,ib}^{(2)}$ happens to have such a value that the quantity

$$\delta = [A(1 - \zeta_{ta,ib}^{(2)}) - B]$$

is small or close to zero, because in this case the interaction connects pairs of levels which in every case are nearly degenerate. Thus there is always appreciable mixing of the two interacting basis functions and repulsion of the corresponding energy levels. The situation is illustrated in *Figure 6* for a prolate symmetric top molecule, and in *Figure 7* for an oblate top molecule. This condition is the same as the condition for $\zeta_{ta,ib}^{(2)}$ to have such a value that the Q branch structure coalesces to give a single sharp feature in the centre of the band.

The form of the interaction Hamiltonian is as follows:

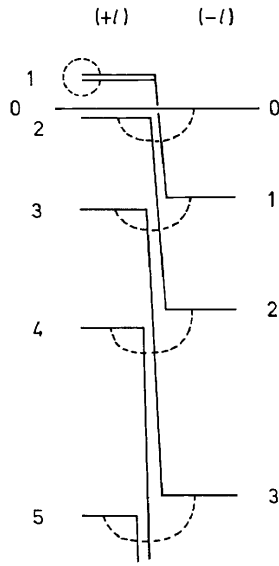
$$\begin{array}{cc} V_l t = 1^{+1} & V_l t = 1^{-1} \\ k + 1 & k - 1 \\ \left[\begin{array}{cc} H_{11} & H_{12} \\ & H_{22} \end{array} \right] \end{array}$$



prolate: $[A(1-\zeta^z) - B] \sim \text{zero}$,

$$\zeta^z \sim +1$$

Figure 6



oblate: $[C(1-\zeta^z) - B] \sim \text{zero}$

$$\zeta^z \sim -1$$

Figure 7

Figure 6. Interaction diagram for *l*-doubling in a prolate top with δ close to zero

Figure 7. Interaction diagram for *l*-doubling in an oblate top with δ close to zero

where:

$$H_{11} = v_t + B_t J(J+1) + (A_t - B_t)(k+1)^2 - 2A_t \zeta_t^{(z)}(k+1)$$

$$H_{22} = v_t + B_t J(J+1) + (A_t - B_t)(k-1)^2 + 2A_t \zeta_t^{(z)}(k-1)$$

$$H_{11} - H_{22} = 4k[A_t(1 - \zeta_t^{(z)}) - B_t] = 4k\delta$$

$$H_{12} = \frac{1}{2} \bar{q}_t [J(J+1) - k(k+1)]^{\frac{1}{2}} [J(J+1) - k(k-1)]^{\frac{1}{2}}$$

It is evident that the interaction will produce an important perturbation whenever H_{12} is large compared to $H_{11} - H_{22}$, and this will tend to become true whenever \bar{q}/δ is large, and also for high values of J and low values of K (i.e., when there is a high angular momentum perpendicular to the top axis). Thus the perturbation will produce the largest effect on the central sub-bands, close to ${}^R Q_0$, and will also produce its largest effect whenever $\zeta_t^{(z)}$ happens to have such a value that δ is close to zero. In practice the effect is most evident in the spectra of oblate symmetric tops, for which \bar{q}/δ is generally larger than for prolate tops.

We have written a computer programme to calculate the band contour of a symmetric top perpendicular band, allowing for the effect of the *l*-doubling

interaction on all the line positions and intensities, by diagonalizing the above matrix for all appropriate values of the quantum numbers. Typical band contours obtained from this programme are shown below in *Figure 12*. It will be seen that the most obvious effect of the perturbation is to produce quite a marked hole in the Q branch structure in the middle of the band, and an asymmetrical distribution of intensity between the P -type and R -type Q branches, the sense of which depends on the sign of the l -doubling constant \bar{q}_t .

The sign of the l -doubling constant is conventionally defined for *linear* molecules by the relation (see Herzberg, Vol. II², p. 378, and Herzberg, Vol. III⁴, p. 70)

$$\bar{q}_t J(J+1) = (\pi^-) - (\pi^+)$$

where π^\pm are vibronic symmetry labels for the interacting levels, this convention being chosen so that \bar{q}_t is positive for the degenerate bending vibration of a triatomic molecule when it is the lowest of the three fundamentals. The accepted convention for *symmetric top* molecules belonging to the C_{3v} point group is to define the sign of \bar{q}_t by the relation

$$\begin{aligned} \bar{q}_t J(J+1) &= (A_1) - (A_2) \text{ for } J \text{ even,} \\ &= (A_2) - (A_1) \text{ for } J \text{ odd,} \end{aligned}$$

where $A_{1,2}$ are rovibronic symmetry labels for the $k = l = \pm 1$ levels which are split in the first order (see Grenier-Besson⁵, Oka⁶, and Herzberg⁴, p. 95). It should be noted that the accepted convention for linear molecules is opposite to that for symmetric tops, if a linear molecule is regarded as a special case of a symmetric top molecule with $k = l$.

Following this convention for the sign of \bar{q}_t in a symmetric top molecule, the effect of the l -doubling interaction on the intensity distribution in a perpendicular band is summarized in the table in *Figure 8*, and the diagrams in *Figure 9*. It will be seen that the effect is always to enhance the intensity of the Q branches on one side of the band centre, and deplete the intensity of

Intensity effect of l -doubling interaction for \bar{q} positive				
ΔK		ΔJ		
Sub-band		P	Q	R
high v	}	e	d	e
R type for + ve δ , P type for - ve δ				
low v	}	d	e	d
P type for + ve δ , R type for - ve δ				
		$\delta = A(1 - \zeta) - B$	— prolate	
		$\delta = C(1 - \zeta) - B$	— oblate	

Figure 8. Intensity perturbations in l -doubling

BAND CONTOUR AND l -DOUBLING EFFECTS

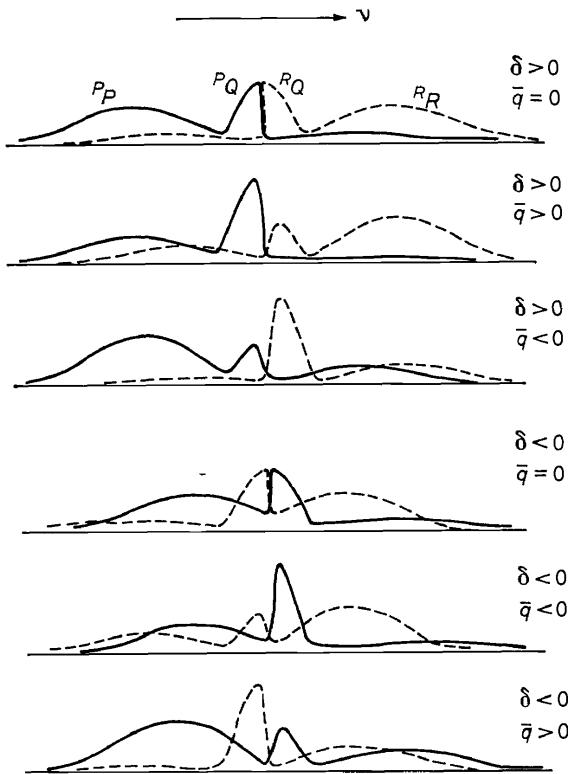


Figure 9. Diagrammatic representation of intensity perturbations in l -doubling interactions: the contour for P -type sub-bands is shown solid, and for R -type sub-bands is shown broken

the Q branches on the other side; moreover where the Q branches are enhanced the corresponding P and R branches are depleted, and vice versa. The sense of these effects depends on the sign of the l -doubling constant \bar{q}_l , and the sign of δ , as indicated in Figures 8 and 9. It should be noted that reliable band contours for various different values of the parameters can only be obtained by writing a computer programme for the correct evaluation of all the line positions and intensities; the band contours sketched in Figure 9 should be regarded as very approximate. Nonetheless they do draw attention to the fact that the perturbation to the overall intensity contour is complicated, and naive interpretations of the band contour, such as those implied in the determination of zeta constants from apparent P and R branch maximum separations, are liable to be seriously in error.

Our discussion thus far has been based on the assumption that the l -doubling interaction arises purely from the effect of the Van Vleck transformation on the xy axis Coriolis interaction terms with a single parallel band. In fact there are three types of contribution which are of comparable importance, which may be referred to as $\bar{q}(\text{cor})$, $\bar{q}(\text{harm})$, and $\bar{q}(\text{anh})$, arising from Coriolis interactions, purely harmonic terms, and anharmonic terms in the complete Hamiltonian respectively. The origin of these terms

	J^0	J^1	J^2
κ^0	$\Sigma \frac{1}{2} [P_r^2 + \lambda_r Q_r^2] = \Sigma \frac{1}{2} \hbar c v_r [p_r^2 + q_r^2]$		
κ^1	$\Sigma k_{rst} q_r q_s q_t$		
κ^2	$\Sigma k_{rstu} q_r q_s q_t q_u + \Sigma \left[\frac{\hbar^2}{2I_{\alpha\alpha}^e} \right] \left\{ \pi_\alpha^2 \right.$	$-2\pi_\alpha J_\alpha$	$\left. + J_\alpha^2 \right\}$
κ^3	$-\Sigma \left[\frac{\hbar^2 a_r^{(\alpha\beta)}}{2I_{\alpha\alpha}^e I_{\beta\beta}^e} \right] \left\{ \begin{array}{c} \text{shaded block} \\ \text{shaded block} \end{array} \right.$	$-Q_r (\pi_\beta J_\beta + \pi_\alpha J_\alpha)$	$\left. + Q_r J_\alpha J_\beta \right\}$
κ^4	$\begin{array}{c} \text{shaded block} \\ \text{shaded block} \end{array} + \Sigma \left[\frac{3\hbar^2 a_r^{(\alpha\xi)} a_s^{(\beta\xi)}}{8I_{\alpha\alpha}^e I_{\beta\beta}^e I_{\xi\xi}^e} \right] \left\{ \begin{array}{c} \text{shaded block} \\ \text{shaded block} \end{array} \right.$	$\begin{array}{c} \text{shaded block} \\ \text{shaded block} \end{array}$	$\left. + Q_r Q_s J_\alpha J_\beta \right\}$

$\kappa = (m/M)^{\frac{1}{4}}$ parameters: λ_r k_{rst} k_{rstu}
 $I_{\alpha\alpha}^e$ $\xi_{r,s}^{(\alpha)}$ $a_r^{(\alpha\beta)}$

Figure 10. Diagrammatic representation of the rovibration Hamiltonian expanded in powers of κ . Shaded blocks indicate terms which are not explicitly given

may be seen from the expression for the complete rovibration Hamiltonian, which is represented diagrammatically in Figure 10, based on a power series expansion of the coefficients, discussed by Oka⁶. The terms in the Hamiltonian are arranged in a table such that the coefficients of terms in successive rows of the table are of decreasing order of magnitude in the expansion parameter $\kappa = (m/M)^{1/4}$, where (m/M) is the ratio of the mass of an electron to the mass of a nucleus. Successive columns in the table are arranged in increasing powers of the dimensionless rotational angular momentum operators J_α , where $\alpha = x, y$ or z . Thus they give rise to terms with a corresponding power dependence on the rotational quantum numbers J or K . Also Q_r and P_r denote the usual normal coordinate and conjugate momentum, q_r and p_r denote corresponding dimensionless normal coordinate and momentum, and π_α denotes the dimensionless vibrational angular momentum about the molecule-fixed α axis ($\alpha = x, y$ or z).

To obtain terms contributing to the l -doubling interaction, satisfying the selection rule $\Delta k = \Delta l = \pm 2$, we require terms containing operators of the type:

$$(\pi_x + i\pi_y)^2 (J_x - iJ_y)^2$$

since this expression can be shown to shift the quantum numbers l and k by two units each, as desired. From the table in Figure 10 we may see where such terms might arise from the Hamiltonian, and what the order of magnitude of the resulting terms in the effective Hamiltonian will be after performing a Van Vleck transformation. Thus the Coriolis contributions, which have

already been discussed, arise from terms of the type $\pi_x J_x$ and $\pi_y J_y$, of order κ^2 , which connect pairs of levels in the E state through an A_1 vibrational state. After performing a Van Vleck transformation, the product of two such terms can obviously contribute in the desired form to the l -doubling interaction, as we have already seen earlier in this discussion; the resulting contribution will be a term of order κ^4 in \bar{q}_t , which we denote $\bar{q}_t(\text{cor})$, and it will appear as a sum over all Coriolis interacting A_1 states. The anharmonic contribution to the l -doubling constant, denoted $\bar{q}_t(\text{anh})$, arises from a combination of cubic anharmonic terms, of order κ^1 and power J^0 , with terms of the type $Q_r J_\alpha J_\beta$ of order κ^3 and power J^2 ; an appropriate combination of such terms through a Van Vleck transformation can evidently contribute to \bar{q}_t a term of order κ^4 , of the same magnitude as $\bar{q}_t(\text{cor})$. Thus the anharmonic contribution will depend on parameters of the type $a_r^{(\alpha\beta)} = (\partial I_{\alpha\beta} / \partial Q_r)$, and on cubic anharmonic constants k_{rst} . Finally there is a harmonic contribution to the l -doubling constant arising from terms of the type $Q_r Q_s J_\alpha J_\beta$ of order κ^4 and power J^2 , which provide a direct interaction between the l -doubling pairs of levels in a degenerate vibrational state. This harmonic contribution depends only on derivatives of the moments of inertia of the type $a_r^{(\alpha\beta)}$. The final expression for the l -doubling constant in a C_{3v} molecule can be shown to be as follows⁶:

$$\bar{q}_t = \bar{q}_t(\text{cor}) + \bar{q}_t(\text{harm}) + \bar{q}_t(\text{anh}),$$

where

$$\bar{q}_t(\text{cor}) = \frac{2B^2}{v_t} \left[\sum_{s \subset A_1} \frac{3v_t^2 + v_s^2}{v_t^2 - v_s^2} (\zeta_{s,ta}(y))^2 - \sum_{s \subset A_2} \frac{3v_t^2 + v_s^2}{v_t^2 - v_s^2} (\zeta_{s,tb}(y))^2 \right]$$

$$\bar{q}_t(\text{harm}) = - \frac{2B^2}{v_t} \left[\frac{3(a_{tb}(y^2))^2}{4I_{zz}} \right]$$

$$\bar{q}_t(\text{anh}) = \frac{2B^2}{v_t} \left[\frac{4\pi c^{\frac{1}{2}}}{h^{\frac{1}{2}}} \left\{ \frac{3k_{tatata} a_{ta}(yy)}{v_t^{\frac{1}{2}}} + \sum_{r \subset E} \frac{k_{tatata}' a_{ta}'(yy) v_t}{v_t'^{3/2}} \right\} \right]$$

The advantage of writing the expression in this form is that each of the terms in square brackets can be shown to be dimensionless and of the order of magnitude 1, so that the dimension and magnitude of \bar{q}_t is given directly as $(2B^2/v_t)$.

For other point groups rather similar expressions are obtained, as given by Oka⁶ and Grenier-Besson⁵. From these expressions we can see that once the harmonic force field of a molecule has been established, it should in principle be possible to obtain information on the anharmonic constants from observed values of the l -doubling parameters \bar{q}_t .

It should also be noted that, of the various contributions to \bar{q}_t , only the Coriolis terms appear with a resonance denominator: this corresponds to the fact that only in this case can the intermediate level, through which the l -doubling interaction occurs, become approximately degenerate with the E vibrational state. When such an accidental degeneracy occurs it is evident that *one* term in $\bar{q}_t(\text{cor})$ will dominate, and will provide the major contribution to the whole l -doubling perturbation (this is what Nielsen and co-workers call 'giant l -type doubling'). In such a case the Van Vleck treatment is

obviously inappropriate, and it would seem best to treat the (3×3) Hamiltonian for the interacting levels exactly, as was done by di Lauro and Mills in the CH_3F bands¹ which I mentioned at the beginning of the lecture.

EXPERIMENTAL RESULTS

I should like to devote the remainder of my lecture to showing examples of observed and computed perpendicular band spectra of symmetric top molecules, to illustrate the effect of l -doubling on the band contour. Most of these examples are chosen from perpendicular bands of the cyclopropane molecule, C_3H_6 , and I must express my thanks to Dr. J. L. Duncan who provided us with most of the observed spectra which are shown in the following diagrams. Cyclopropane has four infrared active perpendicular fundamentals, in the E' species of the D_{3h} point group, conventionally numbered ν_8 through ν_{11} ⁷; the three lowest of these show the effects of l -doubling, which we have tentatively analysed using our band contour programme, to obtain the results shown in *Table 1*. I should like to emphasize that all the parameters shown in this table are *tentative*, in that I am reporting work on fitting these band contours which we have only carried out in recent weeks and which is not yet complete.

Table 1. Perpendicular infrared fundamentals in cyclopropane, C_3H_6

	ν_0/cm^{-1}	$\zeta_{t_1, t_2}^{(z)}$	δ/cm^{-1}	\bar{q}_t/cm^{-1}	Approximate description
ν_{11}	868	-0.95	+0.15	+0.003	ring deformation
ν_{10}	1028	-0.073	-0.246	+0.002	CH_2 wag
ν_9	1437	+0.105	-0.293	-0.003	CH_2 scissors
ν_8	3024	(no l -doubling effect observed)			

Ground state rotational constants: $B'' = 0.6696 \text{ cm}^{-1}$; $C'' = 0.4204 \text{ cm}^{-1}$

Figure 11 shows the best observed and computed spectra for the ν_{11} fundamental of cyclopropane at 868 cm^{-1} . The band centre in the computed contour is essentially at the bottom of the 'hole' in the central Q branch structure. In this case there is a complication in that the observed spectrum is believed to include a weak parallel band centred at *ca.* 853 cm^{-1} (ν_7 , CH_2 rock) which has not yet been included in our calculated spectra. The observed spectrum does indeed show an extra feature at this point which could be the parallel band Q branch; however it seems clear that ν_7 must be very much weaker than the perpendicular fundamental ν_{11} . On the face of it the presence of a nearly accidentally degenerate parallel band should invalidate the Van Vleck type of treatment of the l -doubling interaction on which our computed contour is based; however preliminary normal coordinate calculations which we have made (using the $\zeta_{ta, tb}^{(z)}$ constants as additional data) suggest that the $\zeta_{7, 11a}^{(y)}$ is in fact close to zero, so that despite the near degeneracy of ν_7 the corresponding contribution to \bar{q} (cor) is not unduly large.

Figure 12 shows a series of computed spectra for various positive values of \bar{q}_{11} , to show the sensitivity of the contour to this parameter. It is evident that

BAND CONTOUR AND *l*-DOUBLING EFFECTS

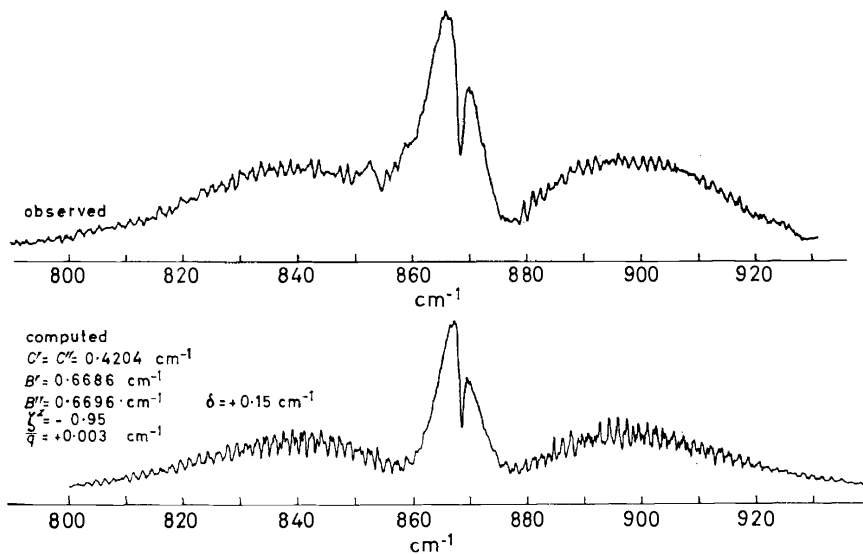


Figure 11. Observed and computed spectra for cyclopropane ν_{11} (868 cm^{-1})

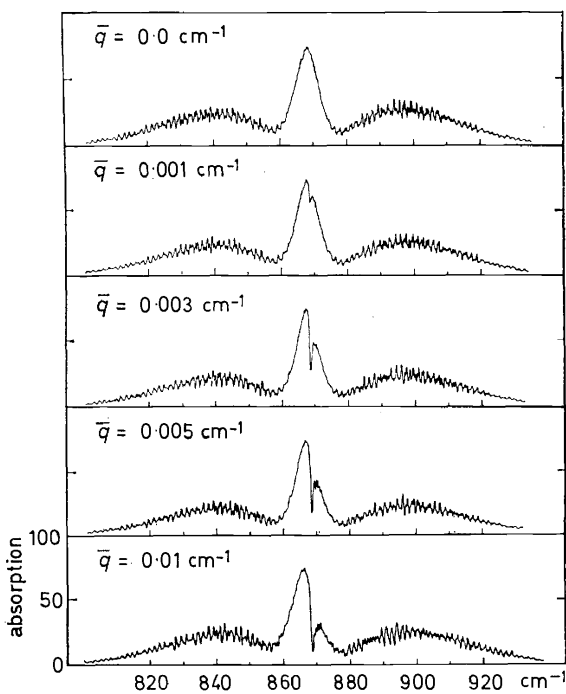


Figure 12. Various computed spectra for cyclopropane ν_{11} (868 cm^{-1})

$$\begin{aligned}
 C' &= 0.4203 \text{ cm}^{-1} & C'' &= 0.4204 \text{ cm}^{-1} \\
 B' &= 0.6686 \text{ cm}^{-1} & B'' &= 0.6696 \text{ cm}^{-1} \\
 \zeta_{11}^z &= -0.95 \\
 [C'(1 - \zeta) - B'] &= 0.15 \text{ cm}^{-1} = \delta
 \end{aligned}$$

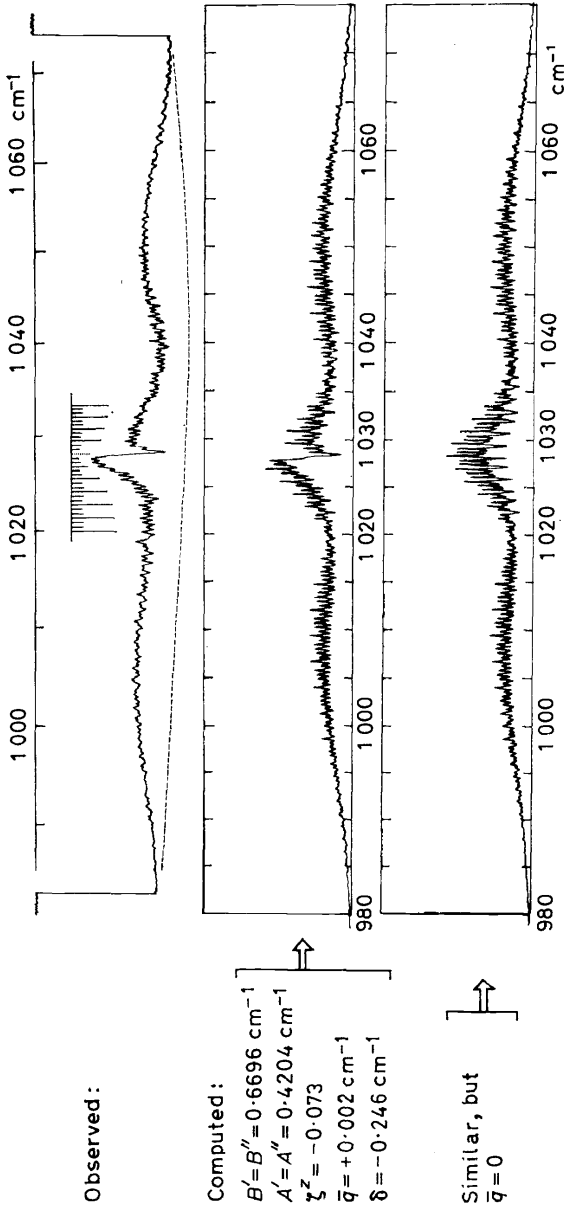


Figure 13. Observed and computed spectra for cyclopropane ν_{11} (1028 cm^{-1})

\bar{q}_{11} can only be obtained with an accuracy of $\pm 15\%$ from band contour analyses of this type. Reversing the sign of \bar{q} essentially reverses the sense of the intensity asymmetry between the two halves of the *Q* branch structure on either side of the central hole.

Figure 13 shows observed and computed spectra for the ν_{10} fundamental at 1028 cm^{-1} . At the bottom of the figure a spectrum is shown computed with the same programme and the same values of all parameters except \bar{q}_{10} which has been set equal to zero, to emphasize the importance of the *l*-doubling effect. Figure 14 shows the region close to the band centre of ν_{10} , as observed

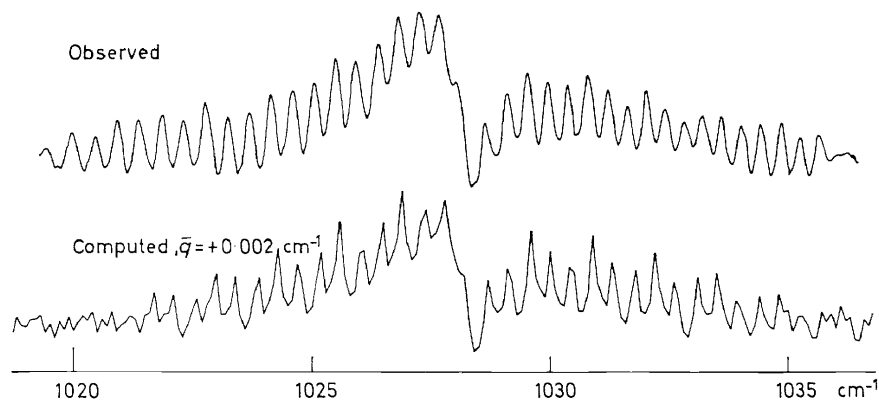


Figure 14. Band centre of ν_{10} at high spread (1028 cm^{-1})

and computed, at high spread, in order to give a clearer picture of the effect of the intensity perturbation on the *Q* branch structure. It will be seen that in this band, where δ is relatively far from zero, the *Q* branch structure is well spread out, so that the individual sub-band *Q* branches are clearly resolved and the three-fold intensity alternation is also quite visible in both the observed and the computed spectra. The RQ_0 branch is the least obvious of all the sub-band *Q* branches, since it occurs as a shoulder on the side of the central hole.

Figure 15 shows observed and computed spectra for the ν_9 fundamental at 1437 cm^{-1} . (The observed spectrum in this case is slightly contaminated with the spectrum of atmospheric water vapour.) In this case again the individual sub-band *Q* branches are clearly resolved, and the intensity alternation is visible. Since the *Q* branches on the high frequency side of the band centre are enhanced we see at once that the sign of the *l*-doubling constant must be positive. In Figure 16 the band centre of the ν_9 fundamental is shown at higher spread, as observed, and as computed.

Figure 17 shows observed and computed spectra for one of the three infrared perpendicular fundamentals of the benzene molecule, C_6H_6 . The band is due to a bending vibration at 1038 cm^{-1} . Again the observed *Q* branch structure shows a marked central hole, and we attribute this to an *l*-doubling effect. The computed spectrum shown in the lower half of the figure was obtained by Dr. di Lauro, working in my laboratory, within the last week. Again the results shown are *very* tentative; in this case there are almost

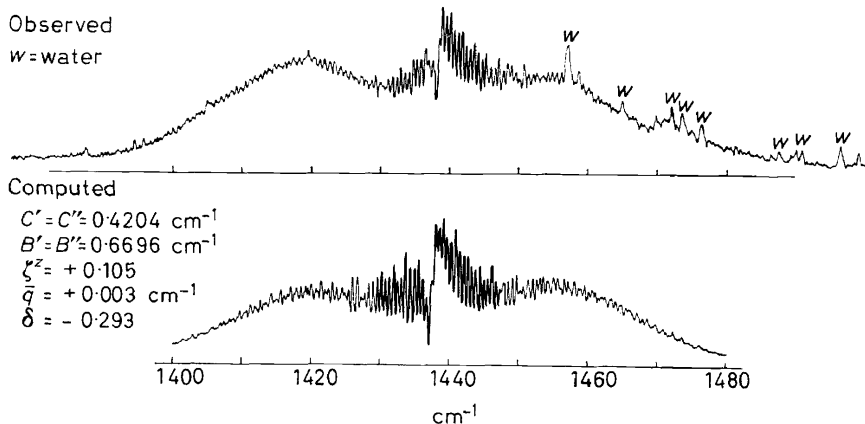


Figure 15. Observed and computed spectra for cyclopropane $\bar{\nu}_q$ (1437 cm^{-1})

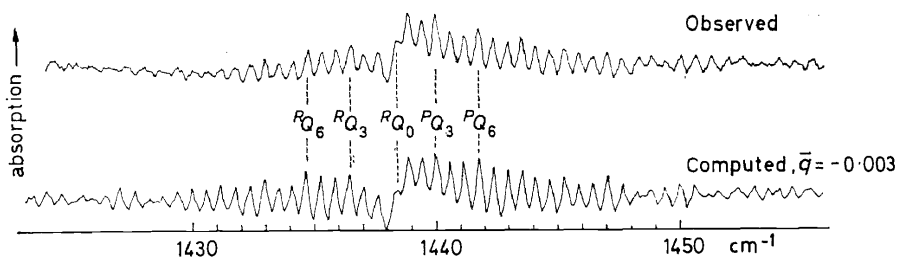


Figure 16. Band centre of $\bar{\nu}_q$ at high spread (1437 cm^{-1})

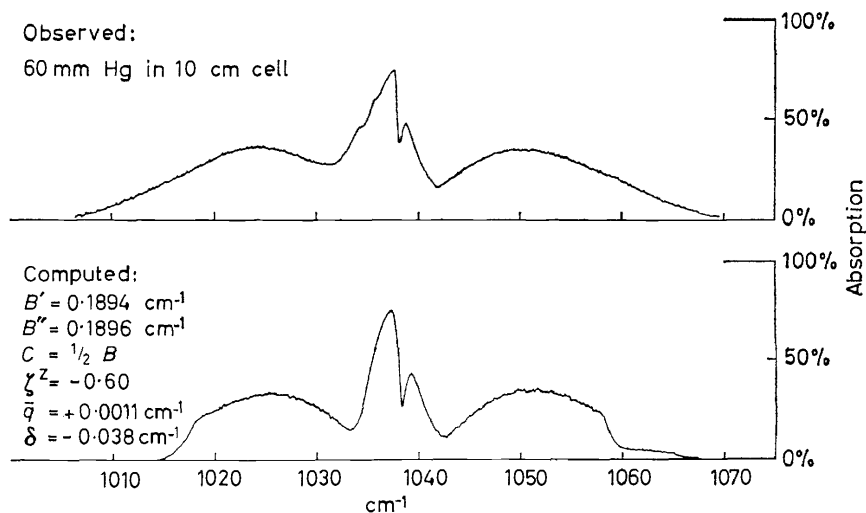


Figure 17. Observed and computed spectra for the 1038 cm^{-1} band of benzene

certainly complications due to the presence of underlying hot bands (which should be relatively unimportant in the cyclopropane molecule). The computed spectrum does show one other interesting feature: owing to lack of computer time, and lack of time before this meeting, the calculations were only carried up to $J = 60$, with the result that the *P* and *R* branch wings of the band appear to have been chopped off. The interesting feature is that the high *P*-type *R* branch lines can be seen beyond the cut-off of the high *R*-type *R* branch lines, in the region of 1060 cm^{-1} , whereas the corresponding *R*-type *P* branch lines are not visible on the low frequency side of the band. This is due to the enhancement of the *P*-type *R* branches that goes with the depletion of the *P*-type *Q* branches, on the high frequency side of the *Q* branch structure close to 1040 cm^{-1} .

I hope that these results demonstrate that numerically quite small values for *l*-doubling constants can produce remarkably large perturbations to the observed rotational band contours of perpendicular bands in oblate symmetric top molecules. We believe that it should be possible to find many more examples of this phenomenon, and it should be possible to determine a number of *l*-doubling constants with reasonable accuracy; I am hopeful that this should provide a new source of information on the force field of polyatomic molecules, as well as providing an explanation of what would otherwise seem to be unexpected features in the observed band contours.

I should like to acknowledge my debt to my colleagues at Reading, particularly Dr. G. J. Cartwright who did most of the work on which this paper is based, and Dr. J. K. G. Watson, and also Dr. T. Oka at the National Research Council in Canada, from whom I have come to understand much of the theory connected with this subject.

References

- ¹ C. di Lauro and I. M. Mills. *J. Mol. Spectry.* **21**, 386 (1966).
- ² G. Herzberg. *Infrared and Raman Spectra* Vol. II, Van Nostrand, New York (1945).
- ³ J. H. Van Vleck. *Rev. Mod. Phys.* **23**, 213 (1951).
- ⁴ G. Herzberg. *Electronic Spectra of Polyatomic Molecules* Vol. III, Van Nostrand, New York (1966).
- ⁵ M. L. Grenier-Besson. *J. Phys. Radium* **21**, 555 (1960).
- ⁶ T. Oka. *J. Chem. Phys.* To be published.
- ⁷ H. Gunthard, R. C. Lord and T. K. McCubbin, Jr. *J. Chem. Phys.* **25**, 768 (1956).